ESTIMATION OF THE UNCERTAINTIES OF THE ORBITAL LIFETIME OF SPACE DEBRIS

D. K. Skoulidou[1], **F. Letizia**[2], **and S. Lemmens**[1]

[1]*ESA/ESOC, Robert-Bosch-Str. 5, 64293 Darmstadt, Germany, Email: {despoina.skoulidou,stijn.lemmens}@esa.int*
[2]*IMS Space Consultancy at ESA, Robert-Bosch-Str. 5, 64293 Darmstadt, Germany, Email: francesca.letizia@esa.int*

ABSTRACT

The IADC mitigation guidelines suggest the end-of-life disposal of a GEO satellite in near-circular graveyard orbits above the GEO protected region, where the perigee altitude is beyond 235 km plus a factor accounting for the solar radiation pressure perturbations. The reflectivity coefficient, C_r, could be around 1.3, but, in general, decreases with time. The aim of this study is to investigate if the default $C_r = 1.3$ is sensible, and how the GEO satellites which are known to have been disposed since 1999 are behaving.

Keywords: geosynchronous; artificial satellites; reflectivity coefficient; uncertainties.

1. INTRODUCTION

The population of space debris at the circumterrestrial region is continuously increasing and the risk for collision with operational satellites is an open issue, especially in the densely populated sub-regions. The motion of the objects is mainly affected by Earth oblateness, lunisolar perturbations, solar radiation pressure and atmospheric drag. Numerous dynamical studies of the near Earth region, and more detailed studies in specific sub-regions, show the physics of satellites' motion, and based thereon the dynamical orbital lifetime can also be roughly estimated. However, for mission design, compliance analysis, and for collision avoidance analyses an accurate orbital lifetime estimation with uncertainty quantification is needed.

The atmospheric drag and solar radiation pressure (SRP) play significant roles mainly in the Low Earth Orbits (LEO) region and in higher altitudes, respectively. Both forces depend on the mass and the area of the object, whereas the atmospheric drag also depends on the atmospheric density. The last decade or so, several studies were performed for the estimation of the ballistic coefficient (BC) which leads to temporal drag coefficient estimations, and as a consequence to variations in lifetime estimations [8][7][4].

In this study, we examine the SRP perturbations and the uncertainties on reflectivity coefficient, C_r, with focus on the Geosynchronous Earth Orbit (GEO), which have a semimajor axis of about $r_{GEO} = 42165$ km. The importance of the GEO region required satellite operators to take measures at their missions' end-of-life phase, already since the very first missions to GEO orbits. The Inter Agency Debris Coordination Committee (IADC) set mitigation guidelines for decommissioning GEO spacecraft [5] and the European Space Agency (ESA) set instructions for the ESA-operated GEO missions [3]. The guidelines, for the disposal of a spacecraft placed in GEO, suggest the disposal in near-circular graveyard orbits above the GEO protected region (super-GEO region), where the altitude of perigee is of the form

$$\Delta H = 235 \text{ km} + 1000 \cdot C_r \frac{A}{m}, \tag{1}$$

where C_r and A/m are the reflectivity coefficient and the aspect area to dry mass ratio $\left(m^2 kg^{-1}\right)$, respectively, and an eccentricity $e \leq 0.003$. The actual value of C_r depends on the surface characteristics, the exposed areas, and the vehicle attitude with respect to the Sun; it may be in range of about 1.2 to 1.5, but it is expected to decrease with ageing [5].

In this study, we investigate if the default $C_r = 1.3$ is sensible, and how the disposed GEO satellites are behaving. In section 2, we describe the choice of the examined population and the dynamical model used for the propagation. A subset of our results is presented in section 3, followed by the conclusions in section 4.

2. PROBLEM FORMULATION

2.1. Examined population and initial conditions

The examined population for this study are the GEO objects that were successfully disposed in graveyards orbits, as defined in [2] and consists of 206 objects in total. The orbital and physical characteristics of the population have been retrieved from the DISCOS database [6]. Figure 1

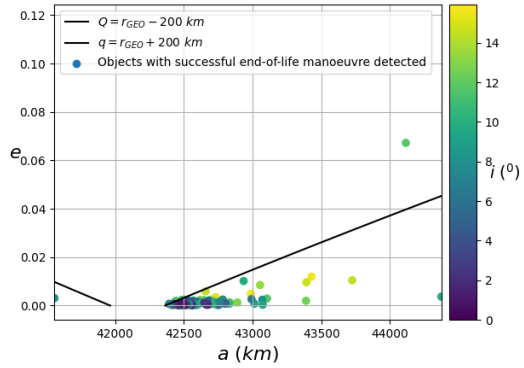

Figure 1: Distribution of the GEO objects that were successfully disposed in graveyard orbits since 1999 in $a - e - i$(colour) phase space. The black lines correspond to the apogee (Q) and perigee (q) values equal to the lower ($r_{GEO}-$200km) and the upper ($r_{GEO}+$200km) limits of the GEO protected region, respectively. The data retrieved from DISCOS database at 05/03/2021.

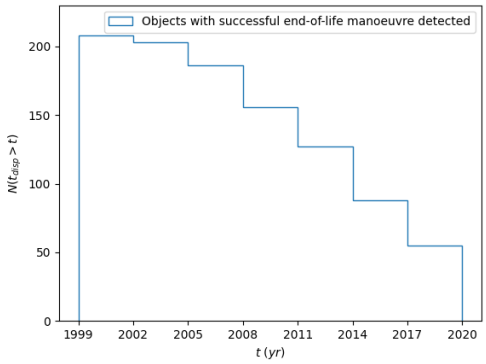

Figure 2: Cumulative distribution of the disposal year of the objects shown in Fig.1.

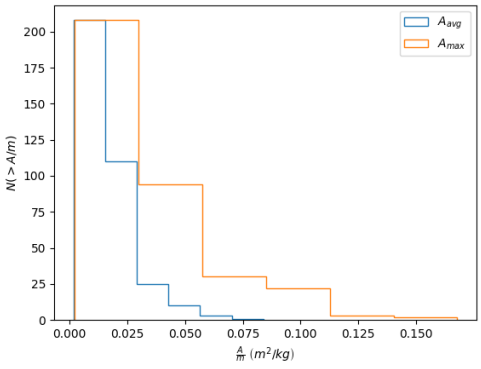

Figure 3: Cumulative distribution of the Area-to-mass ratio, A/m, of the objects shown in Fig.1, as computed using the average cross-section, A_{avg}, (blue), and the maximum cross-section, A_{max}, (orange).

shows the distribution in the semi-major axis - eccentricity - inclination phase space ($a - e - i$(colour)), as retrieved from DISCOS at 05/03/2021. The black lines correspond to the apogee (Q) and perigee (q) values equal to the lower ($r_{GEO}-$200km) and the upper ($r_{GEO}+$200km) limits of the GEO protected region, respectively. Figure 2 shows the cumulative distribution of the disposal year, t_{disp}, of the population, while Figure 3 shows the cumulative distribution of the Area-to-Mass ratio of the population. The blue and orange lines correspond to the average (A_{avg}) and maximum (A_{max}) cross-section, respectively, as provided by the DISCOS database.

Most of the objects are placed beyond the upper limit of the GEO protected region and in low eccentricities ($e < 0.02$). Their inclinations vary in range $0 - 15°$, but this is a classical behaviour of a typical abandoned GEO orbit, with maximum inclination of $15°$ and periodicity of about 53 years. The A/m values of the objects are significant low and typical for Payloads, like the examined objects, where the maximum A/m is double when the A_{max} is used over A_{avg}.

2.2. Propagator and dynamical model

A satellite orbiting around the Earth is affected mainly by the following perturbations: the Earth's oblateness, the higher harmonics of the Earth's geopotential, the lunar and solar gravitational fields, the direct solar radiation pressure and atmospheric drag. The latter particularly affects low-altitude orbits in the LEO region.

In our study, we wish to understand the effect of SRP on the satellite orbits, focusing on the GEO region. For that purpose, we use the orbit propagator FOCUS-2 included in OSCAR of the ESA DRAMA suite, which performs the integration of the singly averaged Gauss variational equations for Keplerian elements. The target orbit to introduce to OSCAR is defined by singly averaged Keplerian elements (i.e., the input should be in terms of mean elements)[1].

The default dynamical model taken into account in the OSCAR propagator is the geopotential up to 6 degree and order $(J_{6,6})$ using Goddard Earth Model GEMT1 , lunisolar perturbations, Solar Radiation Pressure (SRP) defined by the cannonball model + a cylindrical shadow (no Earth flattening for shadow), acceleration due to atmospheric drag from NRLMSISE-00 model, and solar and geomagnetic activity compliant with ISO 27852:2016 / ECSS-E-ST-10-04C: the latest prediction's-method.

We also use CSTATE, an auxiliary tool of ESA DRAMA suite which allows to perform conversions between different coordinate frames and time systems, as well as several orbit theories, to convert osculating to mean elements[1]

[1]The data provided in DISCOS are expressed in osculating orbital elements, while the mean orbital elements are used as input in OSCAR. Hence, we convert the data from DISCOS from osculating to mean el-

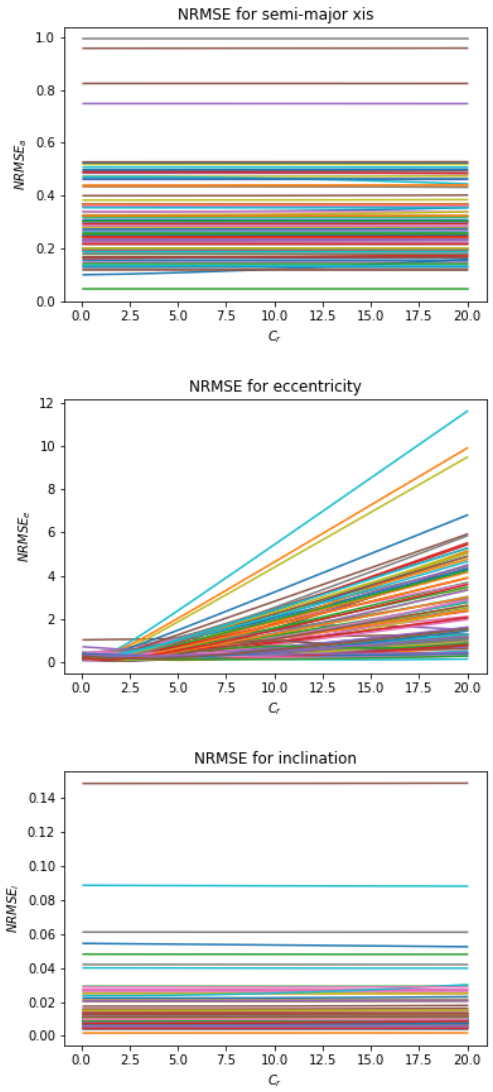

Figure 4: NMRSE vs. C_r of the semi-major axis, a, (top), the eccentricity, e, (middle), and the inclination, i, (bottom). One curve for each of the examined objects. Please see text for more details.

2.3. Initial conditions and data analysis

For each of the examined objects, the orbital state vector at the first available date in the year after the disposal, $t_{disp} + 1\ yr$, as well as the average cross-section and the mass, all provided by the DISCOS database, are used as (the fix) input for the propagations with OSCAR. The sensitivity analysis was performed on C_r, where 200 values were chosen within the range $[0.01, 20]$ with step of 0.01. Please note that the cannonball model itself, which is used to define the SRP, only expects C_r values between 1 and 2 [9]. In this study, a wide range of C_r values are examined, as the differences in evolution are expected to be more pronounced at higher C_r values. The drag coefficient, C_d, was set equal to 2.2 for all cases and has no real influence near GEO. The time-span of the propagation with OSCAR was 100 years with the output to be every 5 days.

For the data analysis, the *Root-Square-Mean Error*

$$\text{RMSE}_y = \sqrt{\frac{1}{n}\sum_{j=1}^{n}\left(y_{OSC,j} - y_{DIS,j}\right)^2} \qquad (2)$$

and the *Normalised* RMSE,

$$\text{NRMSE}_y = \frac{\text{RMSE}_y}{\left(y_{max,DIS} - y_{min,DIS}\right)} \qquad (3)$$

were computed for a, e, and i, where:

- y stands for the variables of a, e, or i
- j stands for the j^{th} epoch provided by OSCAR's output. The NRMSE is computed for n epochs in total, where n stands for the n^{th} epoch provided by OSCAR's output and is closer to the latest epoch from which the DISCOS data were retrieved.
- $y_{OSC,j}$ stands for the OSCAR value of y at the j^{th} epoch (predicted value)
- $y_{DIS,j}$ stands for the mean DISCOS value of y, between the j^{th} and $(j+1)^{th}$ epochs, as it might be more than one entries in DISCOS at this time interval ("real" value)
- $y_{min,DIS}$ and $y_{max,DIS}$ are the minimum and the maximum values of the y variable provided by DISCOS

We further restrict our study for those objects with $t_{dis} = [1999, 2011]$, $96/206$ in total, as for these cases n is large enough for the computation of the RMSE/NRMSE.

3. RESULTS

3.1. Results on C_r distribution

In this section, the results on the C_r distribution for all the examined objects are shown. Figure 4 shows the NRMSE vs. C_r, of a (top), e (middle), and i (bottom), where one curve is for each object of the examined population (i.e., 96 objects in total). Figure 5 shows two examples of evolution of a (1^{st} subplot), e (2^{nd} subplot), and i (3^{rd} subplot) over time, that differs only in C_r, which is equal to 1.3 (left), and 4.8 (right), respectively. Blue and green colours are for the OSCAR output and the DISCOS data, respectively.

According to the results, the NRMSE_a and NRMSE_i values are too close for all the C_r values and for all the

ements and then use them for the comparison with results exported by OSCAR.

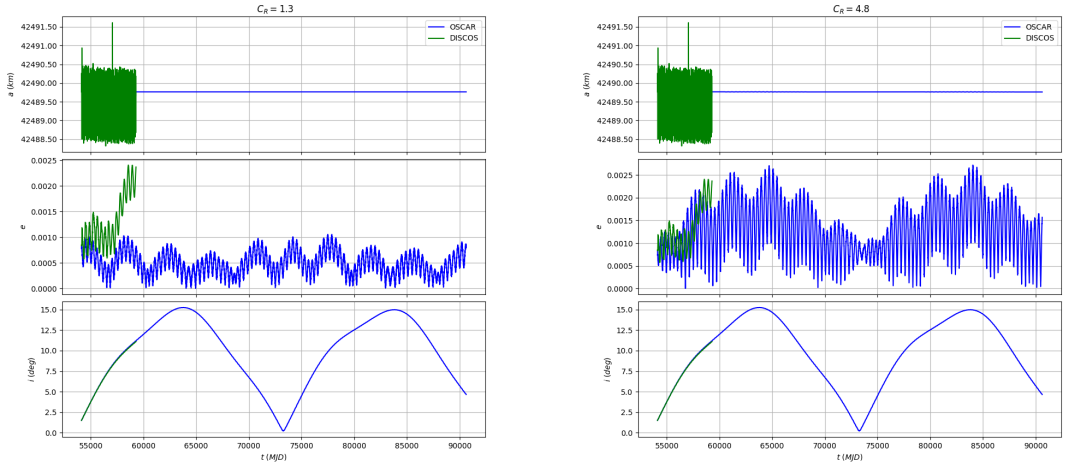

Figure 5: Evolution of a (1^{st} subplot) , e (2^{nd} subplot) , and i (3^{rd} subplot) over time for one examined object, when $C_r = 1.3$ (left), and $C_r = 4.8$ (right) are assumed, respectively. Blue and green colours are for the OSCAR output and the DISCOS data, respectively.

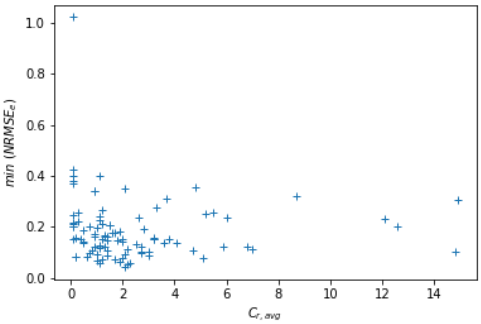

Figure 6: Plot of $C_{r,avg}$ vs. $min\,(NRMSE_e)$ for all the examined population. Please see text for more details.

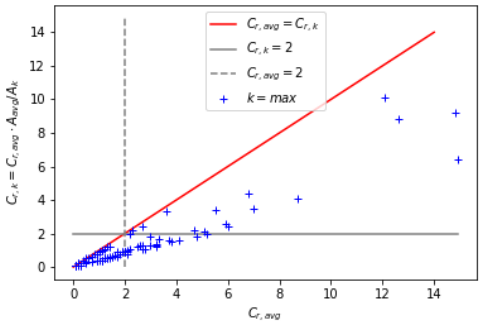

Figure 7: Plot of $C_{r,avg}$ vs. $C_{r,max}$ for all the examined population. Please see text for more details.

examined objects. In the first case, since the equations of motion are averaged over the fast angles, the value of a used as input at OSCAR remains fixed for the total time-span of the propagation, as also is shown in Fig. 5. Hence, we would not expect significant differences on the NRMSE$_a$ as C_r increases. For the NRMSE$_i$, the C_r has limited influence on i. On the other hand, the NRMSE$_e$ significant changes with the variations on C_r for most of the examined objects, as the evolution of e is affected by the SRP perturbations. The maximum NRMSE$_e$ is found for really high C_r values, which tends to 20, and has no physical meaning, but would point to an error in the mass and/or area data for this object in DISCOS. The minimum NRMSE$_e$ is found for various values of $C_{r,avg} \in [0.1, 15]$, as shown in Figure 6. A more detailed analysis is presented in the next section.

3.2. Comparison of the average and the maximum cross-section

It is known that the terms of the equations of motion related to the SRP perturbations are proportional to $C_r \cdot \frac{A}{m}$ [9]. For the simulations performed in this study, the A_{avg} was taken into account and the $min\,(\text{NRMSE}_e)$ was found for an extended range of $C_{r,avg}$ values, where 37.5% and 15.6% of the examined population has $C_{r,avg}$ larger than 2 and 4, respectively.

However, uncertainties on the cross-section and mass could also affect the results. Assuming that the objects' cross-section is A_{max} instead of A_{avg}, we compute the $C_{r,max}$ via

$$C_{r,avg}\frac{A_{avg}}{m} = C_{r,max}\frac{A_{max}}{m}. \quad (4)$$

Figure 7 shows the $C_{r,avg}$ vs. $C_{r,max}$, where grey vertical and horizontal lines correspond to $C_{r,avg/max} = 2$, respectively. In general, it is found that $C_{r,max} < C_{r,avg}$ for all the examined objects. For example, for the object of Fig.5 was found $C_{r,avg} = 4.8$ and $C_{r,max} = 1.8$. The latest value is closer to the default value of 1.3. $C_{r,max}$ is larger than 2 and 4 for the 15.6% and the 6.25% of the examined population, respectively.

A general conclusion could be that the evolution of e can be brought in good agreement. When the A_{max} is assumed, $C_{r,max} < 2$ was found for the most of examined the cases.

4. CONCLUSIONS AND FUTURE WORK

In this study, we examined the uncertainties on C_r for the objects in the GEO region that have successfully disposed in graveyard orbits since 1999. For that purpose, and starting form the first available epoch provided by the DISCOS database the year after the disposal, the OSCAR propagator was used to evaluate the orbits for a 100yr time-span. The cross-section assumed to be the average one. Then, the output from OSCAR was compared with the data retrieved from the DISCOS database by computing the *Normalized Root-Square-Mean Error* for a, e, and i. According to the results, NRMSE was too close for all the examined C_r values for a and i, whereas the same quantity for e gave a minimum value when $C_r \in [0.1, 15]$. The C_r decreases when the maximum cross-section is assumed, but for $\sim 15\%$ of the examined population is still larger than 2. In general, the evolution of e can be brought in good agreement.

The above results could be enriched by examining larger sample of population. Moreover, uncertainties on the cross-section and the mass should also be considered in a future work, as they might affect the C_r findings. The same assessment would also work in MEO around the 2:1 spin-orbital resonance, where the Global Navigation System Satellites (GNSS) are placed in inclined and near-circular orbits and Molniya satellites in inclined and eccentric orbits.

REFERENCES

1. Braun V., Sánchez-Ortiz N., Gelhaus J., Kebschull C., Flegel S., Moeckel M., Wiedemann C., Krag H., Vörsmann P., (2013). Upgrade of the ESA DRAMA OSCAR tool: Analysis of disposal strategies considering current standards for future solar and geomagnetic activity, *In: 6th European Conference on Space Debris*, Darmstadt, Germany, 22-25 April 2013, published by ESA.

2. ESA Space Debris Office (2021). Classification of geosynchronous objects. issue 23, *GEN-DB-LOG-00290-OPS-SD*, ESA/ESOC, Darmstadt, Germany.

3. ESA (2015). ESA space debris mitigation compliance verifications guidelines, *ESSB-HB-U-002*.

4. Haneveer M.R., (2017) Orbital lifetime predictions: An assessment of model-based ballistic coefficient estimations and adjustment for temporal drag coefficient variations. *Master thesis*, Delft University of Technology, Netherlands.

5. IADC (2011). IADC space debris mitigation guidelines, http://www.iadc-online.org/

6. McLean F., Lemmens S., Funke Q., Braun V., (2017). DISCOS 3: An improved data model for ESA's Database and Information System Characterising Objects in Space, *In: 7th European Conference on Space Debris*, Darmstadt, Germany, 17-21 April 2017, published by ESA Space Debris Office.

7. Vey J.P., (2016). Characterization of Space Debris from Collision Events using Ballistic Coefficient Estimation, *PhD thesis*, University of Southern California, USA.

8. Operti A., Braun V., Lemmens S., Corpino S., (2017). Assessing uncertainties in the estimation of the orbital lifetime, *In: 7th European Conference on Space Debris*, Darmstadt, Germany, 17-21 April 2017, published by ESA Space Debris Office.

9. Vallado, D. A. (2013). Fundamentals of Astrodynamics and Applications. Microcosm Press, Hawthorne, CA, 4 edition.